MOISTURE AND TEMPERATURE CHANGES OF WOOD DURING ADSORPTION AND DESORPTION PROCESSES

Tianxin Zhao
Master Candidate
College of Science
E-mail: zhaotianxin.bj@gmail.com

*Erni Ma**†*
Lecturer
College of Materials Science and Technology
E-mail: maerni@bjfu.edu.cn

Wenjie Zhang
Professor
College of Science
Beijing Forestry University
Beijing 100083, China
E-mail: wjzhang@bjfu.edu.cn

(Received October 2012)

Abstract. Sitka spruce (*Picea sitchensis* Carr.) specimens, 10 mm along the grain and 20 mm in radial and tangential directions, were exposed to three different RH conditions of 22, 47, and 75% for adsorption and desorption at 30°C controlled by a self-designed temperature conditioning chamber. Specimen weight was measured and thermal images were taken at certain time intervals during the processes to investigate their moisture and temperature changes. Results showed that at the beginning of the sorption process, moisture content of the specimens changed significantly and their average temperature increased about 2-7°C for adsorption and decreased about 1-6°C for desorption. During adsorption, the temperature for the center section along the longitudinal direction of the specimens was lower than that for the surface section, whereas the opposite was true for specimens under desorption. Along with the adsorption and desorption processes, moisture content and average temperature of the specimens were gradually approaching equilibrium state.

Keywords: Adsorption, desorption, moisture content, temperature, IR thermal imaging.

INTRODUCTION

As a hygroscopic material, wood is greatly affected by moisture content, especially its dimensional stability and mechanical properties. Because of changes in atmospheric RH and temperature, wood is constantly subjected to moisture adsorption (AD) and desorption (DE) (Ma and Zhao 2012). Therefore, it is important to study moisture changes of wood during sorption processes.

Conversely, AD and DE of wood are inevitably accompanied by an exchange of heat or energy (Skaar 1988), which will cause temperature changes of wood at the same time. Because of the movement behavior of moisture during sorption, various studies found moisture gradient occurring in wood (Skaar et al 1970; Jönsson 2004; Ma et al 2010). Therefore, there should be temperature distributions in wood as a result of moisture gradient.

King and Cassie (1940) pointed out that moisture content vs time curves were due to heat dissipation, and the time necessary for moisture equilibrium in the fibers, after a change in

* Corresponding author
† SWST member

environmental conditions, was negligible compared with the time required for dissipation of generated heat. However, Christensen and Kelsey (1959) concluded that the time to reach sorption equilibrium was approximately the same as that to achieve thermal equilibrium. Some studies were also conducted on the temperature changes of wood during sorption processes (Christensen and Kelsey 1959; Kelly and Hart 1970; Engelund et al 2013). However, these limited investigations all used vacuum equipment systems, and little information was available regarding temperature distribution of the specimens.

Temperature changes of wood as a result of heat generated during AD or consumed during DE has not been adequately examined in previous studies because of the lack of scientific, effective, and accurate measuring technology. The IR thermal imager is based on IR radiation detectors and the optical imaging objective principle. It receives energy distribution of a target and reflects it on the photosensitive element of the IR detector, thus obtaining an IR image. Different colors on the thermal image represent different temperatures of the target. Therefore, the surface temperature of an object can be observed by the shooting images (Vadivambal and Jayas 2011). IR imaging is now widely used in medicine, architecture, machinery manufacturing, and other fields (Wright and McGechan 2003; Barreim and Freitas 2007; Meola 2007). In wood science, however, the technology has not received enough attention. Ludwig et al (2004) studied the correlation between moisture content and evaporation of wood samples from their thermal images based on the fact that thermal characteristics of wood were different under various moisture contents because of low heat capacity of the material. Qu and Wang (2009) investigated the application feasibility of IR thermal imaging technology for wood nondestructive testing by analyzing the relationship between timber internal defects and IR radiation field strength.

This study was conducted to 1) observe changes in moisture and temperature of wood during AD and DE processes; and 2) study moisture and temperature distributions in wood and their relationship. The results could not only provide scientific information on temperature changes and distribution during wood sorption, thereby enriching the theory of wood physics, but could also provide a useful index for wood processing based on hydro-thermo treatment and environment-conditioning ability of wood in service.

MATERIAL AND METHODS

Experimental

Sitka spruce (*Picea sitchensis* Carr.) specimens, with dimensions of 10 mm along the grain and 20 mm in both tangential and radial directions, were divided into two groups to be subjected to AD and DE, respectively. The AD group was oven-dried at 105°C, and the DE group was conditioned at 100% RH to the FSP at 30°C. Both groups were moved into a self-designed temperature conditioning chamber.

As shown in Fig 1a, the chamber was made of polypropylene and polymethylmethacrylate, 500 (length) × 300 (depth) × 300 mm (height), with a plexiglass front side for observation. Temperature, with a resolution of 0.05°C and precision of ±0.10°C, was controlled by a microcontroller triggered with a current control circuit. That is, a high-precision temperature sensor was used to measure real-time temperature, and the signal was sent to the microcontroller to regulate the current output, from which the air was heated by a high-power resistor. The proportional-integral-derivative algorithm (Åström and Hägglund 2001), a generic control loop feedback mechanism that attempts to minimize the error by adjusting the process control inputs, was applied to improve temperature stability. Two fans were fixed in the chamber to promote air circulation and ensure temperature uniformity of ±0.3°C. A long-term temperature uniformity is given in Fig 2. Temperature inside the chamber was kept at 30°C throughout the experiment. Three RH conditions of 22, 47, and 75% were selected for both AD

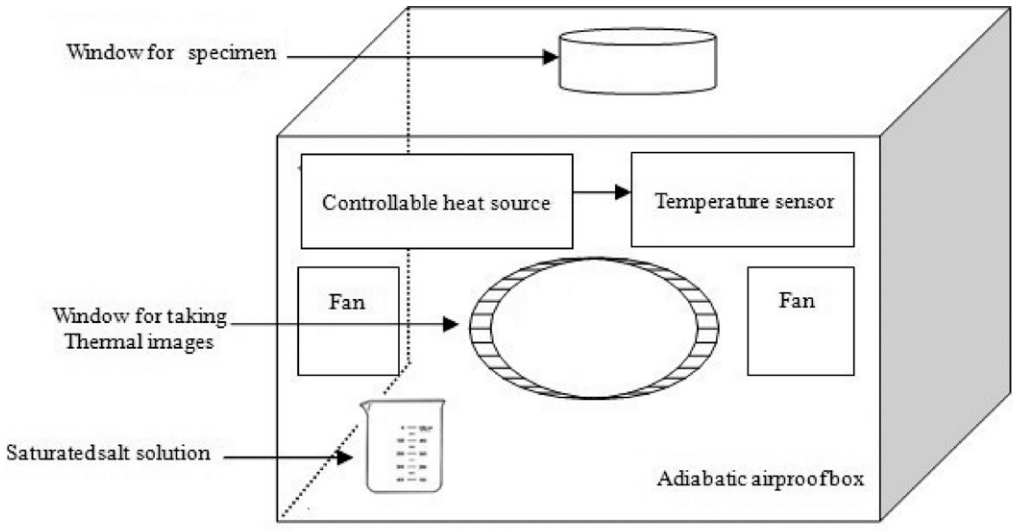

(a)

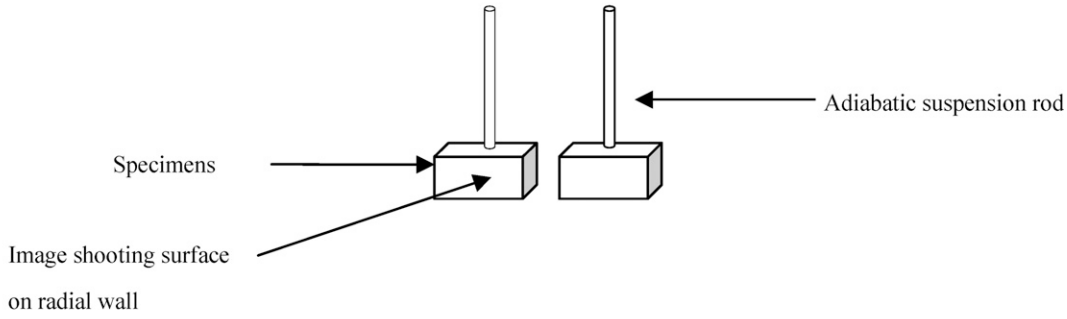

(b)

Figure 1. Schematic diagram showing (a) structure of self-designed temperature chamber and (b) how images were taken and orientation of the specimens.

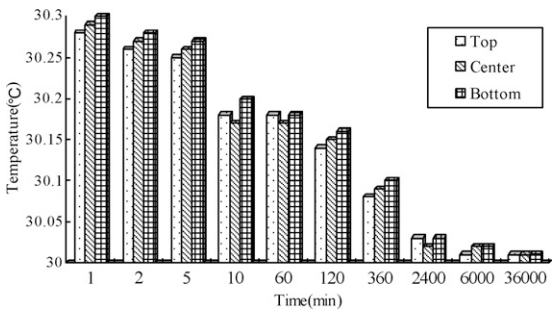

Figure 2. Long-term temperature uniformity estimated at three typical positions, top, center, and bottom, along body diagonal line in the self-designed chamber at 30°C.

and DE controlled by different saturated salt solutions of lithium nitrate ($LiNO_3$), potassium acetate (CH_3COOK), and sodium chloride (NaCl) in three chambers with a uniformity of $\pm 1\%$ RH, respectively (Macromolecule Academy 1958). A temperature and humidity sensor was placed beside the specimens in each chamber to detect temperature and humidity during the sorption processes.

The specimens in the chambers were suspended by adiabatic rods allowing them to be completely exposed to the air (Fig 1b), and IR thermal images of them in the longitudinal direction

on the radial wall were taken at certain time intervals through the front window using an IR thermal imager (FLUKE Ti55; Fluke Corporation, Everett, WA) with thermal sensitivity ≤0.05°C and lens resolution of 320 × 240. After that, the specimens were taken out of the chambers for weight measurement, which was conducted with the weighting bottles capped to prevent the specimens from exchanging moisture with the surrounding environment. Weights were determined to within 0.1 mg. When specimen weight changes within 24 h were less than 0.01% of their oven-dry weights, they were considered to have reached equilibrium. Two specimens, one for AD and the other for DE, were simultaneously used in each of the three chambers. The sorption experiment was repeated three times, and average values of the three tests for temperature and weights of the specimens were taken as the final result.

Theoretical Model for Moisture Sorption

In a previous study (Ma et al 2009), a mathematical model was developed for moisture sorption by wood, and both surface moisture exchange through the air–wood interface and internal diffusion within wood were considered. Moisture exchange on the wood surface is given by

$$m_i = m_{i-1} + a[h - \exp(K_2 K_1^{m_{i-1}}) + K_3]_{i-1}\Delta t \quad (i \geq 1) \tag{1}$$

$$K_1 = 1.0327 - 0.000674T$$
$$K_2 = 17.884 - 0.1432T + 0.0002363T^2$$
$$K_3 = -0.00251$$

where m is moisture content (%), subscripts $i - 1$, i are ordinal time points, a is sorption rate constant (1/h), h is RH for the surrounding atmosphere (%) and T is temperature (K). K_1, K_2, and K_3 are given by the Bradley equation, and their values were validated by experimental isotherm curves, from which K_3 value for Sitka spruce at 30°C was corrected to −0.11. The exponent of K_1, namely $m_{i\text{-}1}$, was converted to 1.087 $m_{i\text{-}1}$ for AD processes and 0.92 $m_{i\text{-}1}$ for DE processes (Ma and Zhao 2012).

For the transfer of moisture inside the wood, a numerical solution by the finite difference method for Fick's second law was used.

$$m_{ji} = \frac{D\left(m_{j-1} - 2m_j + m_{j+1}\right)_{i-1}}{\Delta l^2} + \left(m_j\right)_{i-1} \tag{2}$$

where the subscripts $j - 1$, j, and $j + 1$ are ordinal elements in thickness direction and Δl is thickness of each element (m). D is the moisture diffusion coefficient (m^2/s), and it is calculated by an exponential function for Sitka spruce in the longitudinal direction (Skaar 1988):

$$D = 1.44 \times 10^{-9} \exp(0.11m) \tag{3}$$

In this study, the model was mainly applied to investigate moisture gradient distributions of specimens during sorption. The calculated D was about 1.45×10^{-8} m^2/s, and the value of a, determined when it can give the best fit to the observed data, was 1.4/h, 0.9/h, and 0.8/h for RH of 22, 47, and 75%, respectively.

RESULTS AND DISCUSSION

Moisture Changes and Distribution during Sorption

Moisture changes of the specimens during AD and DE are shown in Fig 3. Figure 3 shows that moisture changes significantly at the beginning of sorption, increasing in the AD group and

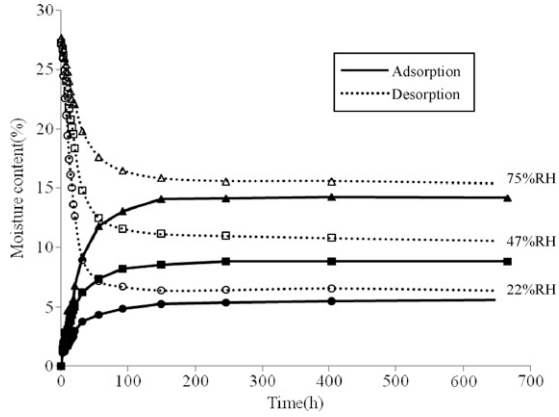

Figure 3. Moisture changes of the specimens during adsorption and desorption processes in different RH conditions.

decreasing in the DE group. Along with sorption, the moisture changes become slight and finally reach equilibrium. In addition, equilibrium moisture content for the AD group is lower than that for the DE group in a given RH, which indicates the sorption hysteresis (Skaar 1988).

Figure 4 gives calculated moisture gradient distributions of the specimens along the longitudinal direction at the very beginning of both sorption processes. In the case of AD (Fig 4a), moisture content of the surface section increased rapidly, whereas that of the middle and center parts almost did not respond to the moistening initially, giving a regular shape of AD distribution (Jönsson 2004). Moisture distributions for DE have the same tendencies as shown in Fig 4b.

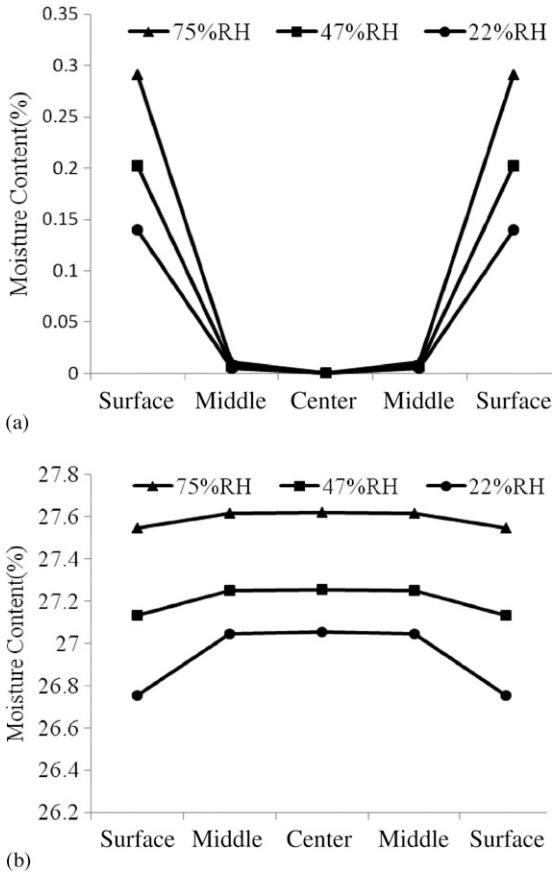

Figure 4. Moisture distributions of the specimens along the longitudinal direction at the beginning of (a) adsorption and (b) desorption in different RH conditions.

Temperature Changes during Sorption

As an example, thermal images of the specimens at the initial stage (120 s) and equilibrium (665 h) of AD and DE in 75% RH are shown in Fig 5. It is clear that, at the beginning of sorption (Fig 5a-b), the temperature of wood changed significantly and took on a gradient distribution in the longitudinal direction based on different colors in the images. However, when the specimens reached equilibrium state (Fig 5c-d), the relatively homogeneous colors indicated uniform distribution of the temperature.

Figure 6 presents temperature changes of the specimens during the first 2 h of AD and DE processes at 75% RH. It can be seen that within 120 s during AD, specimen temperatures increased rapidly and reached a peak value of 37.3°C. Christensen and Kelsey (1959) also found a temperature increase as high as 13°C for small sections (1 mm thick) of *Araucaria klinkii Laulerb* during AD from oven-dry condition to 14% RH. The difference in this temperature increase between their research and this study may have been caused by the absence of air in their study and the variation

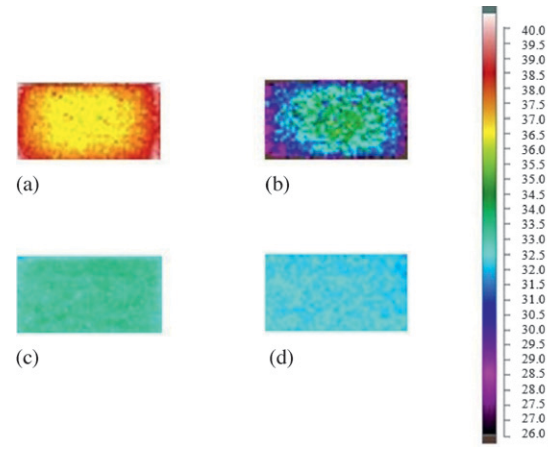

Figure 5. IR images of the specimens for (a) initial adsorption, (b) initial desorption, (c) adsorption equilibrium, and (d) desorption equilibrium in 75% RH.

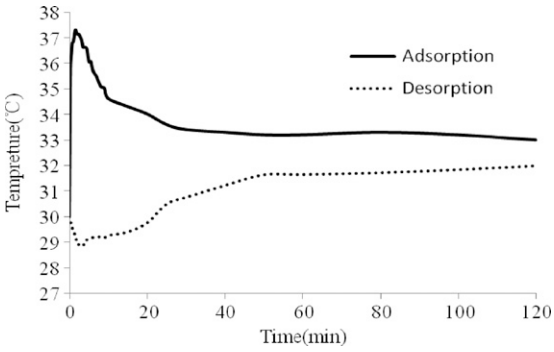

Figure 6. Temperature changes of the specimens in the first 2 h of adsorption and desorption processes in 75% RH.

in size and species of the specimens. The DE group, conversely, showed the opposite. That is, temperature of the specimens decreased quickly and reached its minimum of 28.8°C at the first 180 s of DE. Along with sorption, temperature of the specimens gradually approached equilibrium, maintaining at about 33°C for AD and 32°C for DE.

Figure 7 also gives temperature changes of the specimens during the first 10 min of AD and DE in different RH conditions. Apparently, specimen temperature reached peak value within 120 s during AD in all RH conditions tested (Fig 7a). It is believed that at the very beginning, abundant water vapor in the atmosphere was attracted and bounded to the wood cell wall, which generated heat causing temperature to increase (Skaar 1988). In contrast, DE resulted in the consumption of heat, which lowered wood temperature (Kelly and Hart 1970) (Fig 7b). Also, RH had an effect on the temperature changes of the specimens during sorption. In the case of AD, higher RH caused greater wood temperature increases. Whereas for DE, larger temperature decreases occurred in lower RH.

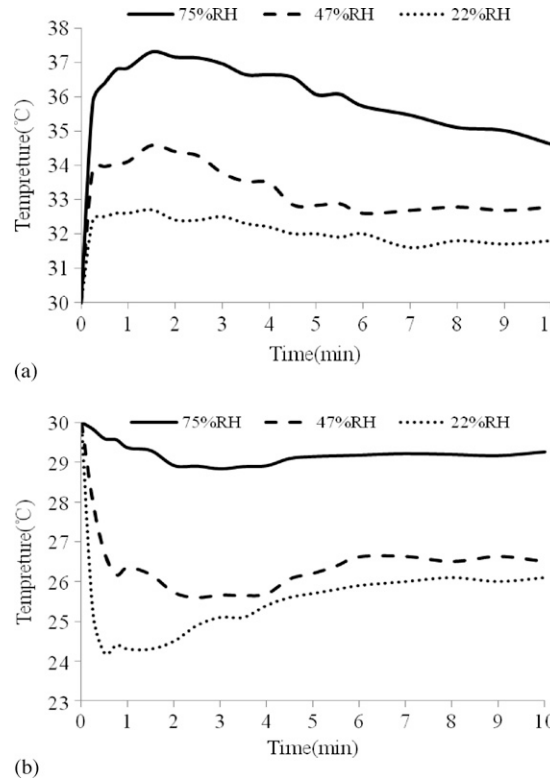

Figure 7. Temperature changes of the specimens during the first 10 min of (a) adsorption and (b) desorption processes in different RH conditions.

Temperature Distribution along the Longitudinal Direction

As indicated in Fig 5, specimen temperature displayed a gradient distribution along the longitudinal direction at the initial stage during sorption. Therefore, five different sections were made in that direction, and their temperatures were estimated based on average values of temperature matrix data exported from the IR images (60 × 6 for each section). The results at the first 120 s of AD and DE are shown in Fig 8 as an example. For AD (Fig 8a), temperature of the center section of the specimens was lower than that of the surface section, and the difference between the two sections was approximately 0.6°C. For DE (Fig 8b), the distributions were reversed. Temperature of the center section was higher than that of the surface section with a difference of about 0.5°C. This may be explained by the moisture distributions of the specimens presented in Fig 4. At the beginning of the sorption process, specimen surfaces were exposed to air allowing them to easily react with water vapor, which caused heat exchanges, whereas the reaction was delayed

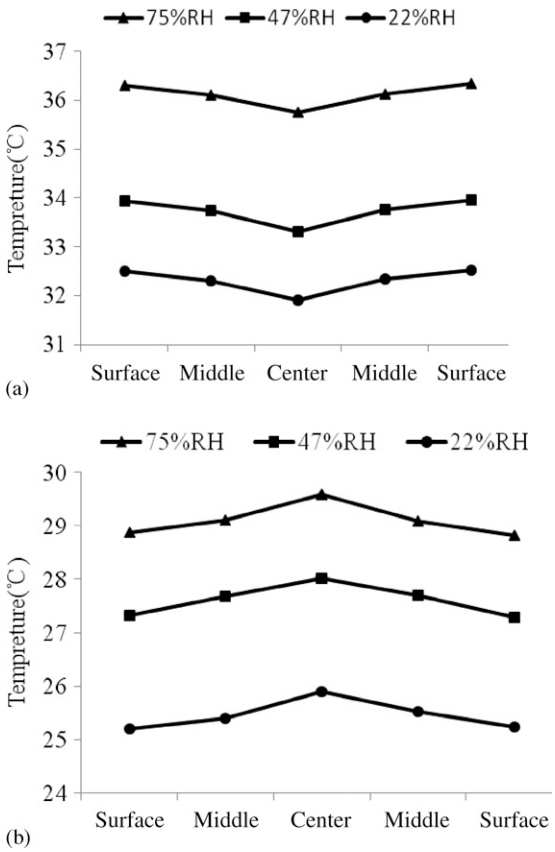

Figure 8. Temperature distribution along longitudinal direction of the specimens at 120 s of (a) adsorption and (b) desorption in different RH conditions.

for the center section, hence the temperature distributions occurred. Also, RH had little effect on the temperature difference between the surface and center section.

CONCLUSIONS

In this study, a self-designed temperature chamber was used to investigate moisture content, temperature changes, and distribution of Sitka spruce exposed to three different RH conditions of 22, 47, and 75% for AD and DE at 30°C. The results mainly showed the following:

1. Moisture content changed significantly at the beginning of sorption and then gradually approached equilibrium state.
2. Temperature of the specimens increased about 2-7°C and decreased about 1-6°C at the very beginning of the AD and DE processes, respectively. Along with sorption, temperature changes gradually reached equilibrium. RH had a positive effect on specimen temperature during sorption.
3. Temperature of the specimens displayed a gradient distribution along the longitudinal direction, and temperature of the center section was lower than that of surface section during AD, whereas DE showed the opposite. RH had little effect on temperature difference between surface and center sections.

Furthermore, Barkas (1949) suggested that mechanical stress developed during sorption could alter moisture state of wood. Therefore, there should be certain relationships between temperature changes and mechanical stress as well. In future work, temperature changes of wood during sorption as a result of mechanical stress will be studied as well as the effect of specimen size on them.

ACKNOWLEDGMENTS

We thank the Beijing Forestry University Young Scientist Fund (no. 2010BXL05) for financial support.

REFERENCES

Åström KJ, Hägglund T (2001) The future of PID control. Control Eng Pract 9(11):1163-1175.

Barkas WW (1949) The swelling of wood under stress. HM Stationary Office, London, UK. 104 pp.

Barreim E, Freitas VP (2007) Evaluation of building materials using infrared thermography. Construct Build Mater 2(1):218-224.

Christensen GN, Kelsey KE (1959) The rate of sorption of water vapor by wood. Holz Roh Werkst 17: 178-188.

Engelund ET, Thygesen LG, Svensson S, Hill CAS (2013) A critical discussion of the physics of wood–water interactions. Wood Sci Technol 47:141-161.

Jönsson J (2004) Internal stresses in the cross-grain direction in glulam induced by climate variations. Holzforschung 58(2):154-159.

Kelly MW, Hart CA (1970) Water vapor sorption rates by wood cell walls. Wood Fiber Sci 1(4):270-282.

King G, Cassie ABD (1940) Propagation of temperature changes through textiles in humid atmospheres. 1. Rate of absorption of water vapor by wool fibers. Trans Faraday Soc 36:445-453.

Ludwig N, Redaelli V, Rosina E (2004) Moisture detection in wood and plaster by IR thermography. Infrared Phys Technol 46(1):161-166.

Ma EN, Nakao T, Zhao GJ (2009) Adsorption rate of wood during moisture sorption processes. Wood Res-Slovakia 54(3):13-22.

Ma EN, Nakao T, Zhao GJ (2010) Dynamic sorption and hygroexpansion of wood subjected to cyclic relative humidity changes. Wood Fiber Sci 42(2):229-236.

Ma EN, Zhao GJ (2012) Special topics on wood physics. China Forestry Publishing House, Beijing, China. 90 pp.

Macromolecule Academy (1958) Physical properties of macromolecule. Kyoritsu Press, Tokyo, Japan. 386 pp.

Meola C (2007) A new approach for estimation of defects detection with infrared thermography. Mater Lett 61(3): 747-750.

Qu ZH, Wang LH (2009) Application of infrared imaging technology in the wood non-destructive testing. Forest Engineering 25(1):21-24.

Skaar C (1988) Wood–water relations. Springer-Verlag, Berlin, Germany. 283 pp.

Skaar C, Prichananda C, Davidson RW (1970) Some aspects of moisture sorption dynamic in wood. Wood Sci 2(3):179-185.

Vadivambal R, Jayas DS (2011) Applications of thermal imaging in agriculture and food industry—A review. Food Bioprocess Technology 4(2):186-199.

Wright T, McGechan A (2003) Breast cancer: New technologies for risk assessment and diagnosis. Mol Diagn 7(1):49-55.